$KCuCeTe_4$: A New Intergrowth Rare Earth Telluride with an Incommensurate Superstructure Associated with a Distorted Square Net of Tellurium

Rhonda Patschke, Joy Heising, and Mercouri Kanatzidis*

Department of Chemistry, Michigan State University and Center for Fundamental Materials Research East Lansing, Michigan 48824

Paul Brazis and Carl R. Kannewurf

Department of Electrical Engineering and Computer Science, Northwestern University Evanston, Illinois 60208

Received November 19, 1997
Revised Manuscript Received January 30, 1998

Explorations in the chemistry of complex lanthanide chalcogenides, particularly quaternary systems of the type A/Ln/M/Q (A = alkali metal, Ln = lanthanide metal, M = transition metal, and Q = chalcogen), suggest that phase stabilization is most facile when the transition metal used is a coinage metal, namely Cu. This may be rationalized by the mobile nature of Cu^+ ions, even at low temperatures, which helps diffuse the ion over long distances and facilitates its quick arrival at phase thermodynamic minima. The introduction of Cu into the synthetic chemistry of lanthanide chalcogenides has already produced several quaternary compounds, $K_2Cu_2CeS_4$,[1] $KCuCe_2S_6$,[1,2] $KCuLa_2S_6$,[2] $CsCuCe_2S_6$,[2] $KCuCe_2Se_6$,[2] $CsCuCeS_3$,[2] and $KCuUSe_3$.[2] These findings were quickly followed by a rapid expansion in this area by independent investigators, producing the compounds $BaErAgS_3$[3], $CsCuUTe_3$,[4,6] $CsTiUTe_5$,[4,6] $Cs_8Hf_5UTe_{30.6}$,[4−6] and $BaLnMQ_3$ (Ln = La, Ce, Nd; M = Cu,Ag; Q = S,Se).[7] We have now examined the A/Cu/Ln/Te system and have identified three new compounds, $Rb_2Cu_3CeTe_5$,[8] $K_2Ag_3CeTe_4$,[9] and $KCuCeTe_4$. The latter, which is reported here, is a rare kind of solid-state compound with two different components, each of which can exist independently. This compound exhibits superstructure phenomena attributed to structural distortions associated with long Te−Te bonding interactions.

$KCuCeTe_4$[10] forms a two-dimensional structure composed of two "distinct" layers, $[CuTe]^-$ and $[CeTe_3]$, see Figure 1. Because each layer is known to exist independently, the $KCuCeTe_4$ can be regarded as an intergrowth compound and a more descriptive formula would be $K^+[CuTe]^-[CeTe_3]$. The $[CuTe]^-$ layer can be described as an ideal anti-PbO structure type, made up of ribbon tetrahedral $[CuTe_4]$ units that share edges in two dimensions. The $[CeTe_3]$ layer adopts the $NdTe_3$ structure type[11e] and has nine-coordinate Ce in a tricapped trigonal prismatic environment of Te. The

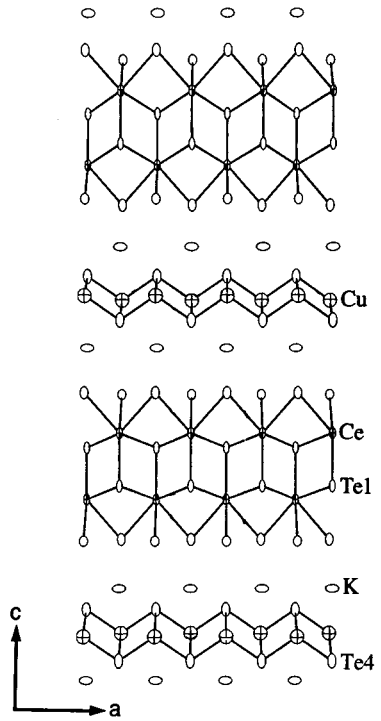

Figure 1. ORTEP representation of the extended structure of $KCuCeTe_4$ as seen down the *b*-axis (90% probability ellipsoids). The ellipses with octant shading represent Ce, the crossed ellipses represent Cu, the large open ellipses represent K and Te. Selected distances (Å) are as follows: Ce−Te1, 3.287(4); Ce−Te2, 3.382(3); Ce−Te3, 3.374(3); Te2−Te3, 3.1417(6); Cu−Te4, 2.667(4); Cu−Cu, 3.1419(6). Selected angles (deg): Te4−Cu−Te4, 108.22(5) and 112.5(2).

* To whom correspondence should be addressed. Fax: (517) 353-1793. E-mail: kanatzid@argus.cem.msu.edu.

(1) Sutorik, A. C.; Albritton-Thomas, J.; Kannewurf, C. R.; Kanatzidis, M. G. *J. Am. Chem. Soc.* **1994**, *116*, 7706−7713.
(2) Sutorik, A. C.; Albritton-Thomas, J.; Hogan, T.; Kannewurf, C. R.; Kanatzidis, M. G. *Chem. Mater.* **1996**, *8*, 751−761.
(3) Wu. P.; Ibers, J. A. *J. Solid State Chem.* **1994**, *110*, 156−161.
(4) Cody, J. A.; Ibers, J. A. *Inorg. Chem.* **1995**, *34*, 3165−3172.
(5) Cody, J. A.; Mansuetto, M. F.; Pell, M. A.; Chien, S.; Ibers, J. A. *J. Alloys Compd.* **1995**, *219*, 59−62.
(6) Pell, M. A.; Ibers, J. A. *Chem. Ber./Recueil* **1997**, *130*, 1−8.
(7) (a) Christuk, A. E.; Wu, P.; Ibers, J. A. *J. Solid State Chem.* **1994**, *110*, 330−336. (b) Wu. P.; Ibers, J. A. *J. Solid State Chem.* **1994**, *110*, 337−344.
(8) Patschke, R.; Brazis, P.; Kannewurf, C. R.; Kanatzidis, M. G., submitted.
(9) Patschke, R.; Brazis, P.; Kannewurf, C. R.; Kanatzidis, M. G. *Angew. Chem.*, submitted.
(10) (a) $KCuCeTe_4$ was synthesized from a mixture of K_2Te (0.500 mmol), Cu (0.125 mmol), Ce (0.125 mmol), and Te (2.0 mmol) that was sealed under vacuum in a quartz tube and heated to 700 °C for 5 days. The tube was then cooled to 400 °C at a rate of 3 °C/h, followed by quenching to room temperature at a rate of 10 °C/h. The excess K_xTe_y flux was removed with *N,N*-dimethylformamide to reveal very thin red-brown plate-shaped crystals in 46% yield, based on Ce. Bulk crystals are moderately water stable, but are air sensitive when finely ground. Microprobe analysis carried out on randomly selected crystals gave an average composition of $K_{1.0}Cu_{1.10}Ce_{1.14}Te_{3.95}$. (b) A Rigaku AFCS6 four-circle diffractometer equipped with a graphite crystal monochromator was used to collect data from a crystal of 0.285 × 0.285 × 0.026 mm^3 dimensions and Mo Kα (λ = 0.71069 Å) radiation. Crystal data at 23 °C: orthorhombic, *Pmmn* (no. 59), $Z = 2$, $a = 4.436(2)$ Å, $b = 4.4498(9)$ Å, $c = 21.304(2)$ Å, $V = 420.5(4)$ $Å^3$, $\rho_{calc} = 5.947$ g cm^{-3}, $2\theta_{max} = 50°$, ω-2θ scan mode, $T = 23°$, 1701 reflections measured, 498 unique reflections, data corrected for Lorentz-polarization effects and for absorption[10c] (based on ψ scans), μ(Mo Kα) = 220.20 cm^{-1}, solution by direct methods using SHELXS-86 software,[10d] anisotropic refinement on F by full-matrix least-squares using the TEXSAN software package,[10e] 30 parameters, $R = 0.064$, $Rw = 0.057$ for 390 reflections having $F_o^2 > 3\sigma(F_o^2)$, min/max residual electron density = −2.77 e^- $Å^{-3}$/4.2 e^- $Å^{-3}$. (c) Blessing, R. H. *Acta Crystallogr.* **1995**, *A51*, 33−38. (d) Sheldrick, G. M. In *Crystallographic Computing 3*; Sheldrick, G. M., Kruger, C., Doddard, R., Eds.; Oxford University Press: Oxford, England, 1985; pp 175−189. (e) Gilmore, G. J. *Appl. Crystallogr.* **1984**, *17*, 42−46.

S0897-4756(97)00760-6 CCC: $15.00 © 1998 American Chemical Society
Published on Web 02/26/1998

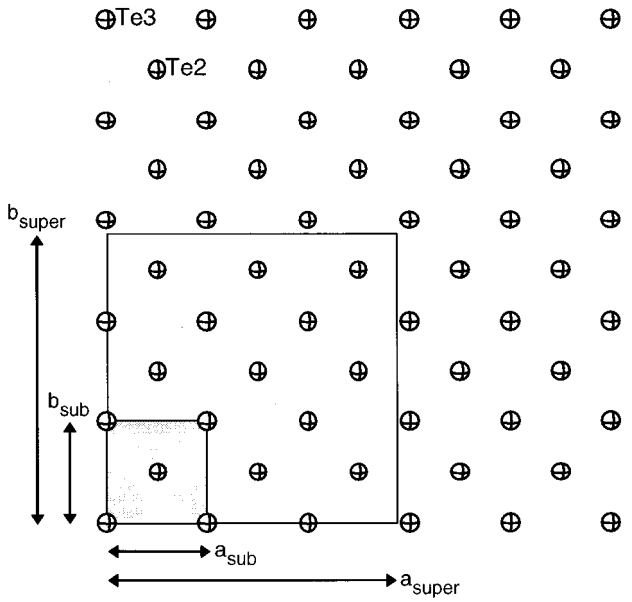

Figure 2. View of the Te "net" in $KCuCeTe_4$ showing the sublattice, determined crystallographically, in the shaded box and the $2.87a \times 2.87b$ superlattice.

$[CuTe]^-$ and $[CeTe_3]$ layers are separated by potassium ions and stack in an A-B-A-B order parallel to the *c*-axis.

The $[CeTe_3]$ layer contains a square Te lattice net. Tellurium square nets are rare and only few are known, e.g., $LnTe_2$, Ln_2Te_5, and $LnTe_3$,[11] $CsTh_2Te_6$,[12] $K_{0.33}Ba_{0.67}AgTe_2$,[13] Cs_3Te_{22},[14] and ALn_3Te_8 (A = Cs,Rb,K; Ln = Ce,Nd).[15] Depending on the electron count, these nets can have different electronic structures, which can lead to instabilities and structural distortions within them.[16] These distortions can lead to interesting physical phenomena such as charge density waves and anomalies in the charge-transport properties. When the formal oxidation state of all Te atoms in the net is −2, a stable square net is observed (e.g., NaCuTe).[17] However, when the formal oxidation state is < −2, or when there are atomic vacancies in the square net, structural distortions are possible leading to Te···Te bonding interactions and the formation of Te_x^{n-} species within the net. These distortions are manifested through the formation of a superstructure with respect to the ideal square net.[18]

The Te net in the $[CeTe_3]$ layer of $KCuCeTe_4$ is fully occupied; see Figure 2. However, the formal oxidation state of the Te atoms in this net is −1, indicating the possibility of a distortion within the Te net. To probe for this distortion we performed electron diffraction studies on $KCuCeTe_4$, which indeed revealed a superstructure lying along the *ab*-plane, which is also incommensurate. The superstructure has a cell of $a_{sup} = 2.87a_{sub}$, $b_{sup} = 2.87b_{sub}$. Figure 3A shows an electron diffraction pattern of $KCuCeTe_4$ along the *ab*-plane. The reflections associated with this superstructure are very weak and occur along both the a^* and b^* directions. A densitometric intensity scan obtained from the (*hk*0) reciprocal plane along the (1*k*0) row of reflections is shown in Figure 3B. The weak reflections between the (1−1 0), (1 0 0), and (1 1 0) reflections are due to the $0.348b^*$ superlattice, which corresponds to a $2.87 \times b_{sub}$ (i.e., ∼13 Å) lattice dimension. These results suggest that there exists a distortion within the Te net of the $[CeTe_3]$ layer, resulting in oligomerization of the Te atoms. Notice that the $[CuTe]^-$ layer also has a square Te net; however, the −2 formal charge on each Te atom is not expected to lead to a distortion and therefore a superstructure. Consequently, the observed superstructure must be localized on the $[CeTe_3]$ part of the compound.

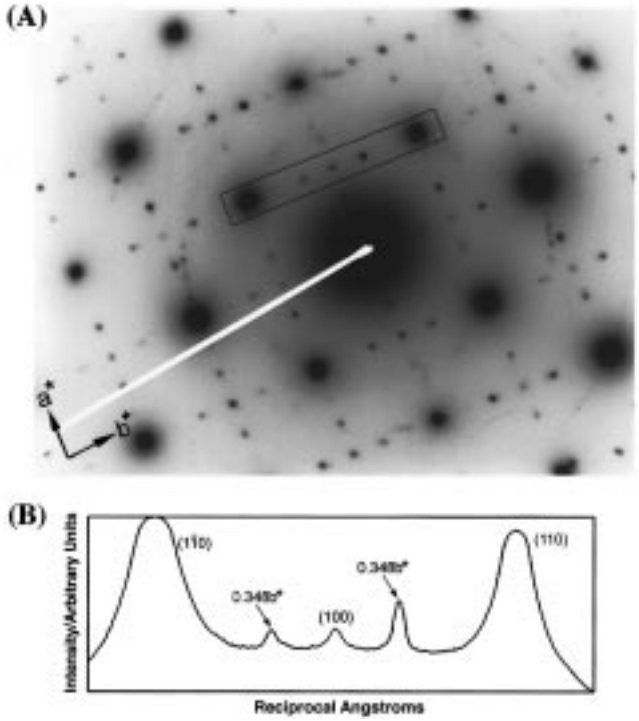

Figure 3. (A) Selected area electron diffraction pattern of $KCuCeTe_4$ with the beam perpendicular to the layers ([001] direction) showing the $2.87a \times 2.87b$ superlattice. (B) Densitometric intensity scan along the b^*-axis of the electron diffraction pattern (boxed area in photograph) showing the (1*k*0) family of reflections. The three reflections from the sublattice of $KCuCeTe_4$ are indexed. The two weak peaks are from the superlattice with $b_{super} = 2.87b_{sub}$.

The magnetic susceptibility of $KCuCeTe_4$ was measured over the range 5−300 K at 6000 G, and a plot of $1/\chi_M$ vs T shows that the material exhibits nearly Curie−Weiss behavior with only slight deviation from linearity beginning below 50 K. Such deviation has been reported for several Ce^{3+} compounds and has been attributed to crystal field splitting of the cation's $^2F_{5/2}$ ground state.[19] At temperatures above 100 K, a μ_{eff} of 2.62 μ_B has been calculated. This value is in accordance with the usual range for Ce^{3+} compounds (2.3−2.5 μ_B).

(11) (a) Lin, W.; Steinfink, H.; Weiss, F. *J. Inorg. Chem.* **1965**, *4*, 877. (b) Wang, R.; Steinfink, H.; Bradley, W. F. *J. Inorg. Chem.* **1966**, *5*, 142. (c) Pardo, M.-P.; Flahaut, J.; Domange, L. C. R. *Bull. Soc. Chim. Fr.* **1964**, 3267. (d) Ramsey, T. H.; Steinfink, H.; Weiss, E. *J. Inorg. Chem.* **1965**, *4*, 1154. (e) Norling, B. K.; Steinfink, H. *Inorg. Chem.* **1966**, *5*, 1488.

(12) Cody, J.; Ibers, J. A. *Inorg. Chem.* **1996**, *35*, 3836−3838.

(13) Zhang, X.; Li, J.; Foran, S.; Guo, H.-Y.; Hogan, T.; Kannewurf, C. R.; Kanatzidis, M. G. *J. Am. Chem. Soc.* **1995**, *117*, 10513.

(14) Wachhold, M.; Sheldrick, W. J. *Angew. Chem.* **1995**, 107, 490.; *Angew. Chem., Int. Ed. Engl.* **1995**, *34*, 2109−2111.

(15) Patschke, R.; Heising, J.; Schindler, J.; Kannewurf, C. R.; Kanatzidis, M. G. *J. Solid State Chem.*, in press.

(16) Lee, S.; Foran, B. *J. Am. Chem. Soc.* **1994**, *116*, 154−161.

(17) Park, Y.; Kanatzidis, M. G., unpublished results.

(18) Zhang, X.; Li, J.; Foran, S.; Guo, H.-Y.; Hogan, T.; Kannewurf, C. R.; Kanatzidis, M. G. *J. Am. Chem. Soc.* **1995**, *117* (42), 10513−10518.

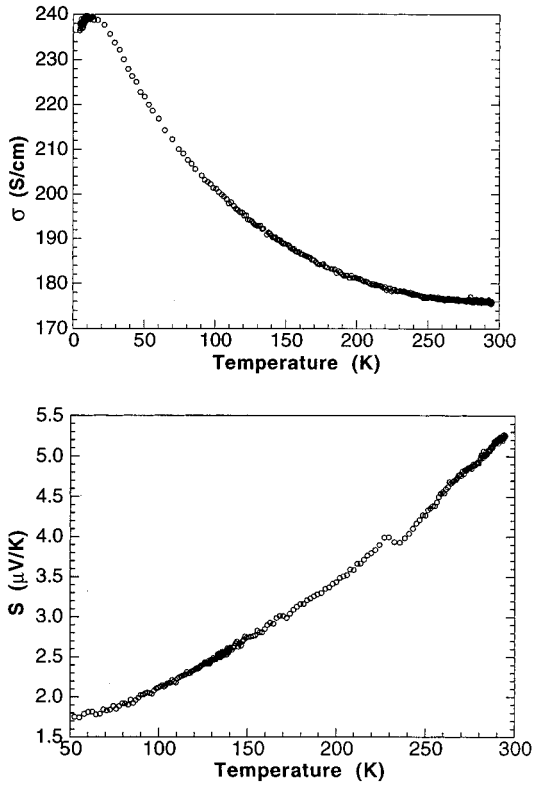

Figure 4. (A) Electrical conductivity data of a hot-pressed pellet of $KCuCeTe_4$ as a function of temperature. (B) Thermopower data of a pressed pellet of $KCuCeTe_4$ as a function of temperature. The discontinuity in the thermopower data around 225 K is a result of residual water vapor desorbing from the walls of the instrument chamber.

Electrical conductivity data as a function of temperature for a hot-pressed (at 200 °C) pellet of $KCuCeTe_4$ show that this material is metallic with a room temperature value of 180 S/cm (see Figure 4). Thermoelectric power data show a Seebeck coefficient at room temperature of ~3 μV/K, which suggests that the carriers are holes. The magnitude and slope of the Seebeck coefficient are consistent with the metallic character of the sample. Therefore, the distortion in the Te layer, which gives rise to the incommensurate superstructure, does not seem to open a gap at the Fermi level of this material. In contrast, a similar incommensurate 3 × 3 superstructure found in $K_{0.33}Ba_{0.67}AgTe_2$[13] leads to semiconducting behavior.

An intriguing fact is the different structure of the $[CuTe]^-$ layer in the compound KCuTe[20] from that found in $KCuCeTe_4$. In KCuTe, a layered boron nitride type structure is seen while the $[CuTe]^-$ layer with the same alkali ion in the quaternary phase adopts the structure of NaCuTe (i.e., anti-PbO). So, in a way, the $KCuCeTe_4$ has enforced a presumably higher energy, metastable, structure on KCuTe by sandwiching it between $CeTe_3$ layers. The driving force for the stability of $KCuCeTe_4$ is therefore unknown unless some electron transfer exists between the two different metal chalcogenide layers.

Acknowledgment. Financial support from the National Science Foundation (DMR-9527347 M.G.K. and DMR-9622025 C.R.K.) is greatly acknowledged. The work at Northwestern made use of the Central Facilities supported by NSF through the Materials Research Center (DMR-9632472). M.G.K. is a Henry Dreyfus Teacher Scholar 1993−1998. This work made use of the SEM and TEM facilities of the center for Electron Optics at Michigan State University.

Supporting Information Available: Tables of crystallographic details, fractional atomic coordinates of all atoms, anisotropic and isotropic thermal parameters of all atoms, interatomic distances and angles, and calculated and observed X-ray powder diffraction patterns (11 pages); table of calculated and observed structure factors for $KCuCeTe_4$ (3 pages). Ordering information is given on any current masthead page.

CM970760H

(19) Greenwood, N. N.; Earnshaw, A. *Chemistry of the Elements;* Pergamon Press: New York, 1984; p 1443.

(20) (a) Savelsberg, G.; Schäfer, H. *Z. Naturforsch* **1978**, *33b*, 370−373. (b) Berger, R.; Eriksson, L. *J. Less Common Met.* **1990**, *161*, 101.